Cool Stars, Stellar Systems and the Sun
ASP Conference Series, Vol. 154, 1998
eds. R. A. Donahue and J. A. Bookbinder

X-Ray Jets and Their Radio Signatures at Metric and Centimeter Wavelenths

L. van Driel-Gesztelyi[1,2], R.F. Willson[3], J.N. Kile[3], A. Raoult[1], L. Klein[1], N. Mein[1], P. Rudawy[4], B. Cader[4], B. Rompolt[4], B. Schmieder[1], P. Mein[1], and J.M. Malherbe[1]

Abstract:

On October 19, 1995 at 10:30 UT and 17:00 UT, two semi-homologous X-ray jets were observed with the *Yohkoh*/SXT from AR 7912, a region having a reversed polarity group with vortex-like Hα fibril pattern and X-ray loops. The jets appeared over a mixed magnetic polarity region in the vicinity of the leading spot.

The first event was also observed with the Nancay radio heliograph at 167, 236, and 327 MHz. Type III activity, indicating the presence of electron beams, superimposed on a noise-storm was clearly visible. Type III activity first appeared at 10:25 UT, coincident with the onset of the X-ray jet, at 164 MHz and 236 MHz close to the storm position, and in the direction of the X-ray jet. At 10:28:40 UT a new group of sources appeared eastward of the former activity, which may correspond to another jet branch along a more easterly path seen in the *Yohkoh* images.

The second X-ray jet event was also observed with the Very Large Array (VLA) at 6.2, 20.7, and 91.6 cm. For this event, VLA snapshot maps at 6.2 and 20.7 cm reveal low-brightness temperature changes in source structure at the site of the X-ray jet during the preburst, impulsive, and decay phases. The VLA 91.6 cm observations also show noise storm emission above the active region but there is no clear temporal correlation between this later X-ray jet and the impulsive decimetric bursts that were observed during this period. Although the X-ray observations show that the two jets had similar temperatures, emission measures, speeds and trajectories they appear to have had dissimilar metric responses to these events. This surprising result may question our understanding of the process of electron beam acceleration in jets.

1. Introduction

The process of magnetic reconnection in the solar atmosphere can lead to the acceleration of particles in a thin current sheet separating regions of opposite magnetic polarity; these energetic particles may escape from the reconnection site and produce characteristic signatures at different heights in the active region.

[1]Observatoire de Paris, Section de Meudon, F–92195 Meudon Principal Cedex, France
[2]Konkoly Observatory, H–1525 Budapest, Pf. 67, Hungary
[3]Department of Physics and Astronomy, Tufts University, Medford, MA 02155, USA
[4]University of Wroclaw, Astronomical Institute, PL 51 622 Wroclaw, ul. Kopernika 11, Poland

For example, if magnetic reconnection occurs at the base of a large, relatively open structure in the chromosphere, cool plasma may be squeezed by untwisting magnetic fields and forced into the corona producing an Hα surge or ejection event (Schmieder et al. 1993). Surge phenomena have been mainly observed using Hα spectroheliograms while more energetic ejection events or "jets" have been detected primarily at X-ray or UV wavelengths. These recurrent events typically last for 10–20 minutes and may occur at the same location within an active region, usually within an area of inverted or satellite magnetic polarity. Canfield et al. (1996) found that Hα surges and hot jets are not co-spatial or interleaved, though they appear co-planar; they concluded that magnetic tension and relaxation play important role in the physical mechanism driving ejections and that surges and jets are products of magnetic reconnection process induced by a moving satellite polarity.

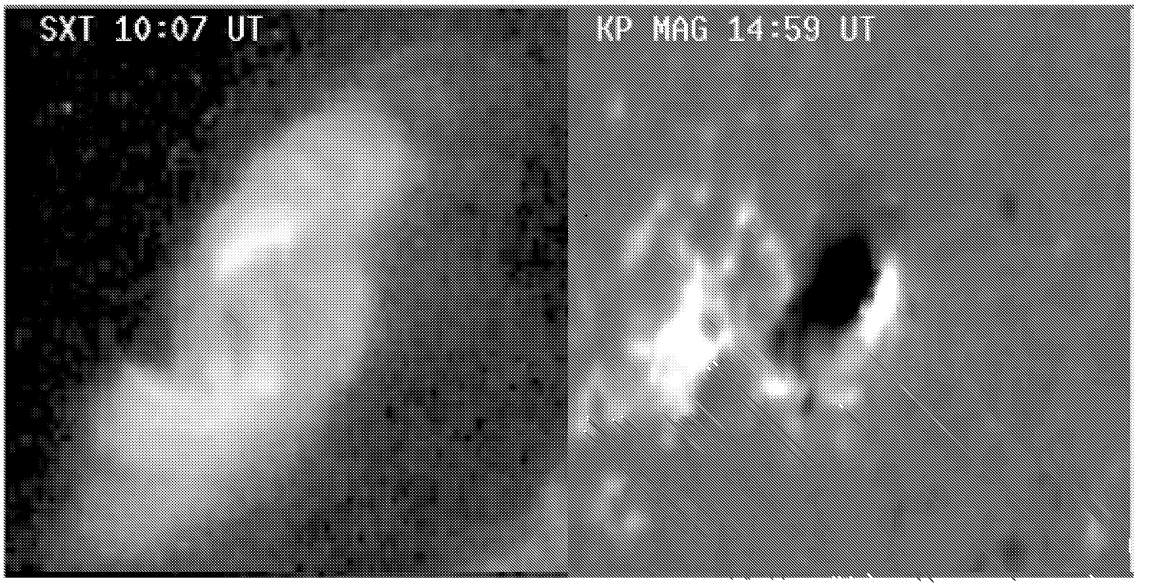

Figure 1. NOAA AR 7912 on Oct. 19, 1995 in the photosphere, chromosphere and corona. Co-aligned images: Kitt Peak magnetic map & white-light image, MSDP Hα line center and off-band ($\pm$ 0.9 Å) images and *Yohkoh*/SXT observations.

Surges or ejected material from the transition region may also produce signatures in other spectral domains including Type III bursts at decimetric wavelengths (Chiuderi-Drago, Mein, & Pick 1986) and coronal heating or sub-flaring in the same or adjacent coronal loop at X-ray wavelengths (Rust, Webb, & MacCombie 1977; Schmieder et al. 1993, 1995). Recently, for example, Kundu et al. (1994) showed that flaring X-ray bright points can give rise to weak (20 solar flux units at 164 and 236 MHz) non-thermal emission in the form of Type III-like radio emission (Nancay Radioheliograph data) from electron beams in addition to thermal soft X-ray emission from the heated plasma. Kundu et al. (1995) and Raulin et al. (1996) have also reported metric Type III bursts in association with soft X-ray jets detected with the *Yohkoh* SXT.

In this paper we compare data from the *Yohkoh* SXT, the Nancay radio heliograph, the Very Large Array, the Meudon Multichannel Subtractive Double

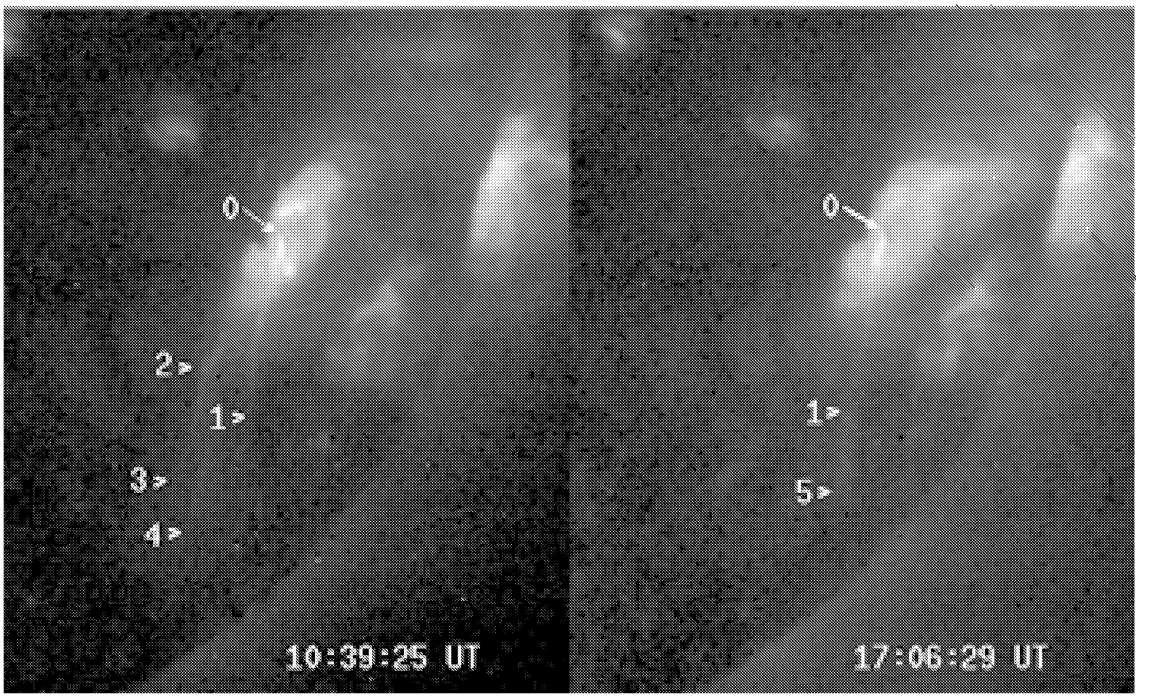

Figure 2. Two semi-homologous X-ray jets and underlying magnetic features. The overlays show that the jets originate from the same location in the AR, namely from the "elbow" of a curved inversion line. The existence of remote jet footpoints appears unlikely, although there is one small bipole (1) which seems to appear under both jet-paths.

Pass spectrograph and Kitt Peak magnetograph to study two semi-homologous X-ray jets. The combined data sets were used to study the structure, evolution and physical parameters of the active region during different phases of each jet.

2. Magnetic Structure of the Target Active Region AR 7912

NOAA active region AR 7912 was a reversed polarity region appearing at the end of the solar cycle in the Southern hemisphere. In general, such regions appear highly non-potential. Indeed, AR 7912 showed a vortex-like appearance in both Hα and soft X-rays (Fig. 1), indicating the presence of strong currents. The active region had a basically bipolar structure with a mixed polarity region to the south of the leading spot. Two small flares of the B GOES level (B3.2 at 10:29 UT and B1.3 at 16:59 UT on Oct. 19, 1995), were observed in the region accompanied by X-ray jets originating from the mixed polarity (basically quadrupolar) area.

It is still an open question whether jets represent plasma flow along open field lines or along closed, far-reaching large-scale loops. If the latter is true, remote magnetic footpoints of the jets should exist. We overlayed the two X-ray jets on a Kitt Peak magnetogram which was rotated to the times of the X-ray pictures. It seems that under the end-points of the jets there were no important magnetic features, which makes the open field-line scenario more likely, though we acknowledge the difficulties arising from projection effects.

3. MSDP (Hα) observations

The evolution of Hα emission associated with AR 7912 on 19 October 1995 was observed with the Meudon Multichannel Subtractive Double Pass (MSDP) spectrograph mounted on the German VTT telescope on Tenerife.

Along the magnetic inversion line on the eastern side of the big spot a filament was observed, which underwent strong changes during and after the 1B/B3.2 flare and jet which started at 10:24 UT. The jet, well observed in the corona, unfortunately was out of the field of view, temporary reduced to the vicinity of the spot, of the MSDP instrument. Also, the observing time with the MSDP ended before the afternoon jet, thus we do not know whether the hot jets were accompanied by surges, (e.g., ejection of cool material) or not.

The MSDP images taken at 10:58:30 UT (large field of view again, see lowest panels in Fig. 1) show the structure of the active region after the flare (the flare ended at 10:43 UT). There are strong redshifts at both ends of filament indicate plasma downflows. Furthermore, a new region of intense redshift (above –20 km s^{-1}) appeared to the east of the filament. It is no wonder that the filament was strongly disturbed by the flare & jet events, since they were centered around the southern end part of the filament where a mixed magnetic polarity region was seen in the Kitt Peak data (Fig. 2).

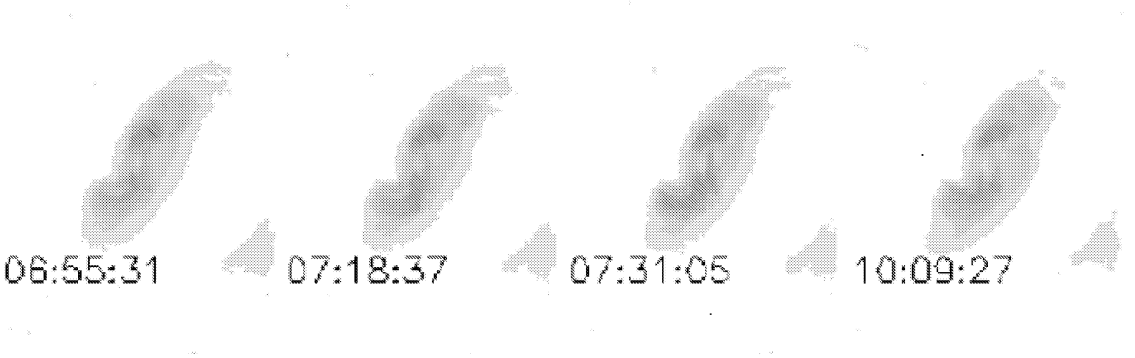

Figure 3. The evolution of the X-ray loop structure of the region with the two jets. Co-aligned and brightness normalized *Yohkoh*/SXT full resolution images (128×128 pixel area, 2.46″/pixel resolution). Note the different level of complexity of the two jets at 10:29 and 17:01 UT.

4. *Yohkoh*/SXT Observations

Figure 3 shows the evolution of the X-ray loop structure of the region with the two jets. The pictures are normalized, thus the changes of brightness between different images are real and not due to different exposure times. With time the loops structure of the AR seems somewhat to expand and there is a new loop brightened by 16:24 UT connecting the AR to some weaker dispersed magnetic fields westward. The first jet at 10:29 UT appears to be brighter than the second one at 17:01 UT. This impression is supported by the study of emission measure of the jet region (see Table 1). The first jet, close to its footpoint, reached about three times higher emission measure than the second one, while

the main body of the jets were not very different neither in emission measure nor in temperature. For the electron densities of the jets along the jet body, but still in the field of view of the partial frame images of *Yohkoh*, with a diameter ≈ 7000 km we got $N_e \approx 4 \times 10^9$ cm^{-3} and $N_e \approx 3.6 \times 10^9$ cm^{-3}, respectively. The jets extended with a speed at least 700 km s^{-1} and reached the length of $2.5 - 3 \times 10^5$ km. The first jet seems to be more complex than the second one, but this might be due to their different brightnesses. In Figure 3 at 10:29 UT besides the straight jet a brilliant curved loop is visible, connecting the footpoint of the jet to the vicinity of a satellite negative polarity on the SW. In fact there were several small-scale X-ray loops involved in the event covering the mixed magnetic polarity area. Also, the large-scale appearance of the first jet was complicated, showing two jet-paths (the middle "jet" existed before the event, thus it is probably a longe-range loop). The second jet looked more simple, and it only had one clear large-scale jet-path, although a faint curved second jet-path towards the East might have been present as well. The second jet was preceded by a loop brightening starting at N–NE to the big preceding spot, which started at 16:50 UT and reached maximum brightness at 16:55 UT, a few minutes before the jet onset.

Table 1. Emission measure and temperature of the two X-ray jets

Oct. 19	Dur.	EM $\times 10^{28}$ cm^{-5}			T (10^6 K)		
1995	min.	flare loops	base of jet	jet	flare loops	base of jet	jet
10:30	15	14.4	8	1.2	11	8	6.5
17:00	10	5.1	2.2	0.9	8	6.5	6.2

5. Nançay Observations

The first event, between 10:25–10:32 UT, was observed with the Nancay radio heliograph at 164, 236, and 327 MHz (Fig. 4). Type III activity superimposed on a noise-storm was clearly visible at 164 MHz, 236 MHz and 327 MHz. At 164 MHz and 236 MHz the noise-storm had a double structure, while at 327 MHz it consisted of a single component. They were likely situated above the AR and their positions appear closer to the limb due to projection effects. Type III activity first appeared at 164 MHz and 236 MHz close to the storm position and in the direction of the X-ray jet. Between 10:28:40 UT and 10:28:50 UT a new group of sources appeared eastward of the former activity, which may correspond to a second jet event along a more eastern path. At 327 MHz burst activity was observed near the position of the storm, and close to the location of the first type III burst, along the X-ray jet.

6. VLA Observations

The VLA was used at 6.2, 20.7, and 91.6 cm between 14:30–19:00 UT on October 19, 1995. At the time of these observations, the VLA was in the B configuration which provided synthesized beamwidths of $1\farcs5$, $5''$, and $22''$ at $\lambda = 6.2$, 20.7, and 91.6 cm. The data were obtained using a time resolution of 3.3 seconds

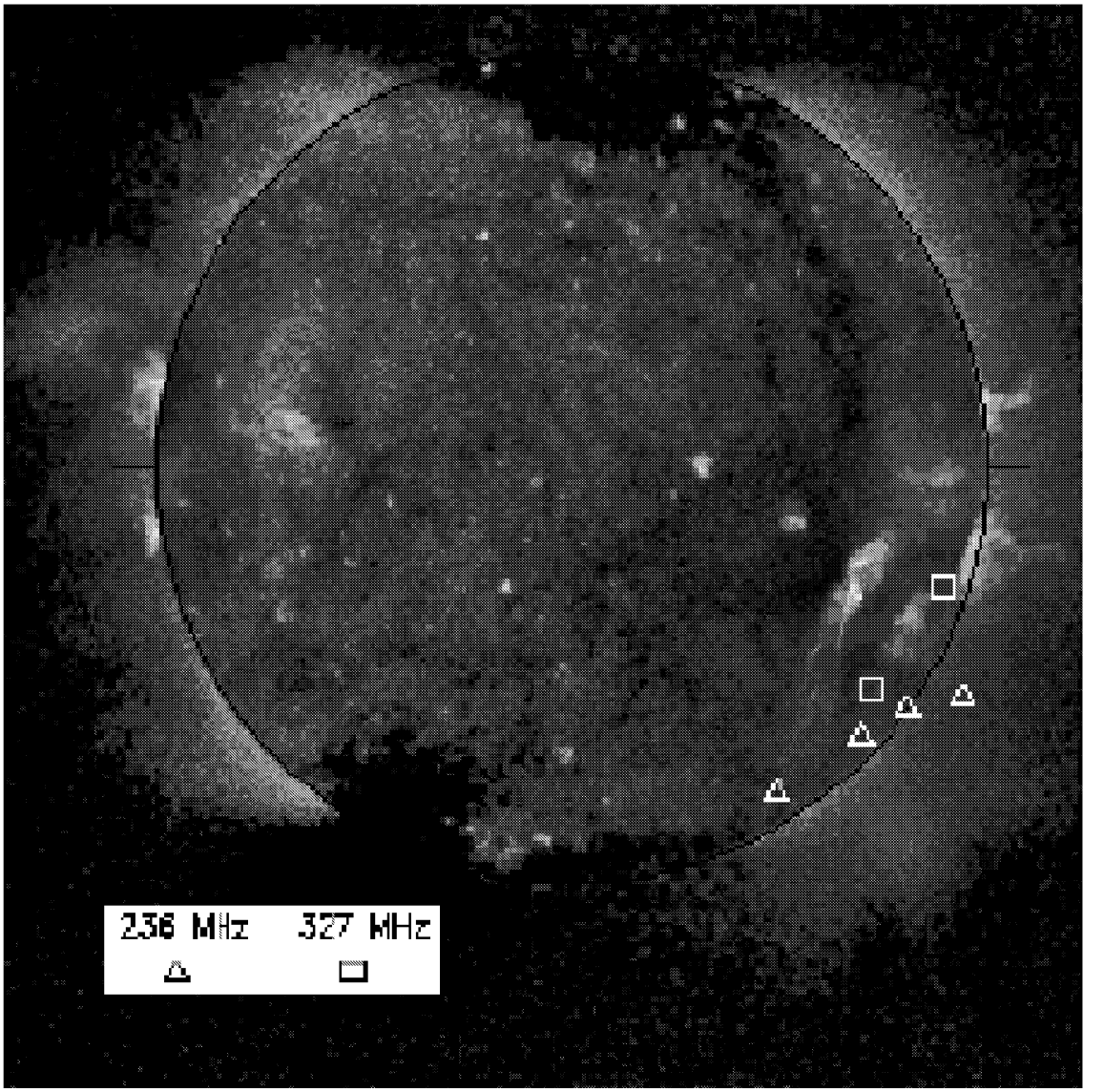

Figure 4. Locations of Nançay radio bursts at 236 and 327 MHz plotted over a *Yohkoh*/SXT image of the first jet. Taking into account projection effects, the radio bursts seem to be related to the jets as well as to the AR itself.

and bandwidths of 12.5 MHz at 6.2 and 20.7 cm, and 3.125 MHz at 91.6 cm. Observations of the full solar disk at 20.7 and 91.6 cm (LP mode) were alternated with observations of AR 7912 at 6.2 cm every 10 minutes for 45 minute periods followed by 5 minute observations of the calibrator source PKS1328+307.

In Figures 5–8 we show VLA images that depict the evolution of the radio emission associated with AR 7912 at the three wavelengths. The 20.7 cm maps show that the emission consists of an elongated source ($\theta_s \approx 1\farcm5 \times 2\farcm5$) whose spatial extent coincides with the soft X-ray emission detected by *Yohkoh*. During the 2.5 hours preceding the X-ray jet event at 16:58 UT, the most intense emission is centered in the northern part of the active regions, with a lower brightness temperature "tail" extending along the X-ray emission to the south.

Figure 5. VLA snapshot maps showing the development of the 20.7 cm emission associated with AR 7912 on 1995 October 19. The contours denote levels of equal brightness temperature with an outermost contour and contour interval equal to $T_b = 2 \times 10^5$K. The field of view of these images is $5' \times 5'$)

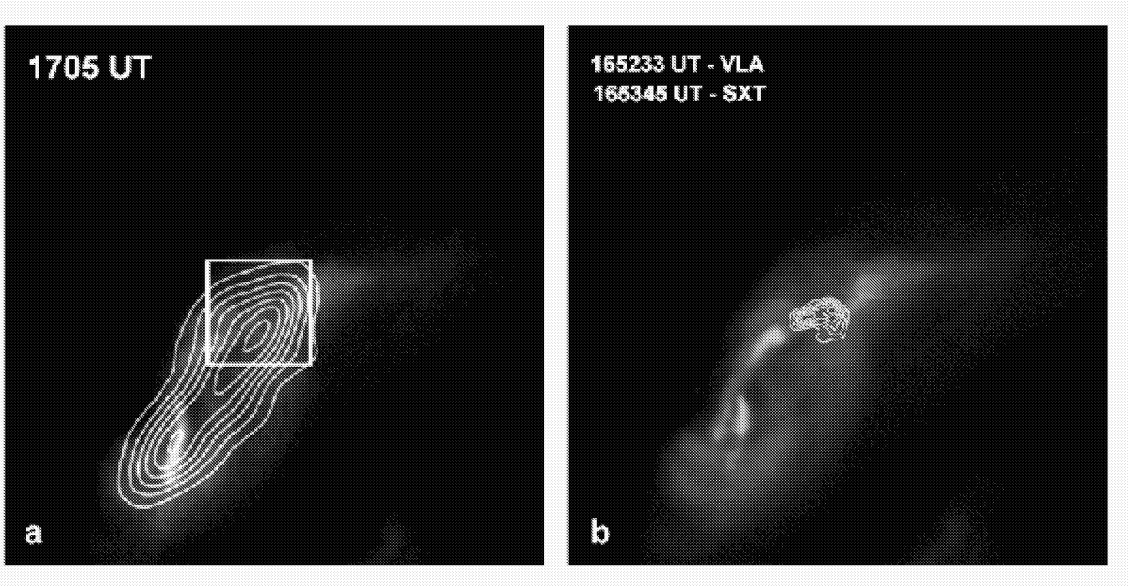

Figure 6. a) A VLA 20.7 cm snapshot map at 17:05 UT is compared with a *Yohkoh* SXT image at the same time. b) A VLA 6.2 cm snapshot map at 16:52:33 UT is compared with a *Yohkoh* SXT image at 16:53:45 UT.

Snapshot maps made during the impulsive phase between 17:01:30 and 17:13:03 UT then show the development of a second intensity peak that appears to coincide with the bright X-ray jet (Fig. 6a). This second component reaches a

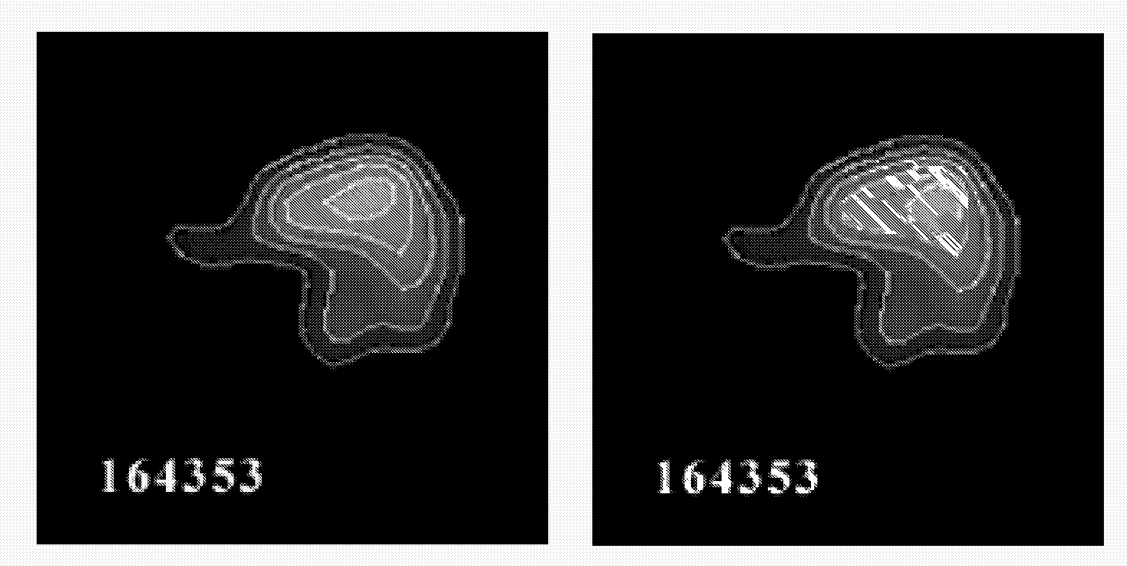

Figure 7. VLA snapshot maps showing the development of the 6.2 cm emission associated with AR 7912 on 1995 October 19. The contours denote levels of equal brightness temperature with an outermost contour and contour interval equal to $T_{\rm b} = 2 \times 10^5$ K. The $1' \times 1'$ field-of-view coincides with the box drawn on the 20 cm map shown in Fig. 8a)

brightness temperature of $\approx 1.3 \times 10^6$ K at approximately 17:08 UT and then gradually decreases in intensity until the source structure once again consists of a single component in the northern portion of the active region.

The 6.2 cm maps (Fig. 7) made between 14:30–16:45 UT show a single, compact ($\theta_{\rm s} \approx 40''$), moderately circularly polarized ($\rho_{\rm c} \approx 40\%$ RCP) source ($T_{\rm b,max} = 1.2 \times 10^6$ K) that coincides with the northern 20 cm source. The relatively high circular polarization suggests that this source is due to thermal gyroresonance or nonthermal gyroresonance of electrons trapped in the high magnetic fields of the nearby sunspot. Subsequent maps then reveal the emergence and growth of a second component about $10''$ to the east of the primary peak, starting as early as 16:45:43 UT. As shown in Figure 6b, this evolving source points in the direction of the bright X-ray loop in the northeast, which started brightening in X-rays at 16:50 UT, but does not coincide with it. This new 6 cm source attains a maximum brightness temperature of $T_b = 1.0 \times 10^6$ K at 16:52:33 and may be the signature of preburst heating of the coronal plasma near the base of the loop a few minutes before the start of the X-ray event. Although the 6.2 VLA beams cover the entire active region, no emission at this wavelength was detected at the site of the X-ray jet event above a brightness temperature of $T_{\rm b} = 1.0 \times 10^5$ K. When the 6.2 cm observations resumed at 17:14 UT, this second component had disappeared, leaving only the main source with about same brightness temperature, size and polarization it had 30 minutes earlier.

Our full-disk 91.6 cm observations show an intense Type I noise storm in progress about $2'$ to the west of AR 7912 (Fig. 8). It is noteworthy that at

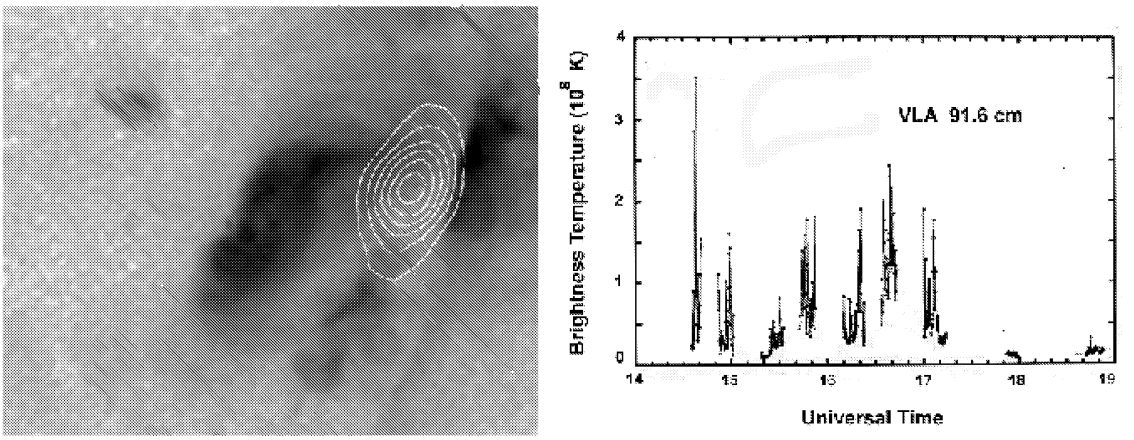

Figure 8. (left) A VLA 91.6 cm snapshot map (3.3 second time interval) at 161923 UT is compared with a *Yohkoh* SXT image taken at the same time. The contours denote levels of equal brightness temperature with an outermost contour and contour interval equal to $T_b = 2 \times 10^7$ K. (right) A plot of the 91.6 cm brightness temperature of the noise storm source associated with AR 7912 on 1995 October 19.

such disk location a source at 0.15 $R_\odot$ height above the AR would appear in projection at the observed source position. Snapshot maps on intervals as short as 3.3 seconds revealed that this source had a relatively low degree of circular polarization ($\rho_c \leq 10\%$) and a nearly constant position (to within $1'$) and angular size ($\theta_s \approx 2' \times 3'$) throughout the day. The source also was highly variable, with frequent, short duration ($\Delta t \leq 3 - 6$ seconds) bursts that reached a brightness temperature as high as $T_b = 3.5 \times 10^8$ K above a more slowly varying level of $T_b = 1 - 2.5 \times 10^7$ K. Figure 8 shows that these impulsive bursts occured throughout the day but that there was no significant change in the brightness temperature of the decimetric emission during the X-ray event, as there was at 20.7 cm. Although the VLA cannot unambiguously distinguish Type III from Type I bursts (by measuring the drift rate of these events) we expect that Type III bursts would have a significantly different brightness temperature, polarization or location than the longer-lasting Type I noise storm emission. Because none of these features were observed during the time of the X-ray jet, we believe that Type III burst emission was not detected at 91.6 cm for this later event.

7. Conclusions

The two X-ray jets observed on Oct. 19, 1995 originated from a reversed-polarity AR over a mixed polarity region close to the leading spot. At least one of the jets had a multiple structure (two jet-paths) indicating the complexity of the magnetic topology.

Our VLA and Nancay observations have revealed several different signatures of particle acceleration during the times of these two X-ray jets. First, the VLA observations at 6 cm show the appearance of a new microwave source at the base of a bright X-ray loop connecting the footpoint of the second jet and the

main sunspot about 5 minutes before the start of the impulsive phase. This new source could, in principle, be due to an increase in the temperature, density or magnetic field strength in this region, or a combination of these. Analysis of the *Yohkoh* data shows indeed an increase in the electron temperature and emission measure of a loop with a footpoint under the radio source during these times. Furthermore, a change in the magnetic field topology might have been produced during the magnetic reconnection event that subsequently led to the ejection of the X-ray-emitting jet plasma.

The VLA 20 cm observations show a gradual increase in the brightness temperature during the peak and decay phase of the second X-ray jet. These changes are consistent with an increase in the electron temperature and emission measure that was observed by *Yohkoh* during this time.

Nancay observations at 164, 236, and 327 MHz reveal Type III bursts during the first jet event along and in the vicinity of the jet paths providing direct evidence for propagating electron beams in the corona. For the second jet, the VLA 91 cm observations show no clear evidence for Type III bursts. Instead, the emission seems to be dominated by a long- lasting Type I noise storm whose position lies close to the site of noise storm detected earlier by Nancay at 327 MHz. The absence of Type III emission is surprising because the two jets had similar speed (around 700 km s^{-1}) and trajectory suggesting that the coronal magnetic field structure along which the Type III-producing electrons travel, was the same for both events. Their different Type III-response may suggest that the process of beam acceleration might not be directly linked to the jet. It should be pointed out, however, that because the VLA observations began during the decay phase of the X-ray jet, we cannot say that Type III bursts were not produced during its early stages, although during the time interval covered by this event there was no type III burst reported in the *Solar-Geophysical Data* either.

Finally, it is interesting to note that the 91 cm noise storm emission associated with the second X-ray jet abruptly ended about 20 minutes after this event (see Fig. 8), at about the same time when *Yohkoh* went into night-mode. Type I noise storm emission is thought to be produced by suprathermal electrons which create plasma instabilities and Langmuir waves that are subsequently converted to ordinary-mode electromagnetic waves at the fundamental of the plasma frequency. The cessation of the noise storm then likely signals a significant change in the excitation conditions or physical parameters – a possible effect of the jet event.

Acknowledgments. Solar radio observations at Tufts University are supported by NASA grant NAGW–5136 and NAGW–2383 and NSF grant ATM 96–13888. We also acknowledge support from the Small Research Grant Program of the American Astronomical Society. LvDG acknowledges the research grant OTKA T17325. We thank the *Yohkoh* Team for the SXT data. The VLA is operated by Associated Universities, Inc., under contract with the National Science Foundation. The NSO/Kitt Peak magnetogram data used in the paper are produced cooperatively by NSF/NOAO, NASA, GSFC, and NOAA/SEL, courtesy Karen L. Harvey.

References

Canfield, R.C., Reardon, K.P., Leka, K.D., Shibata, K., Yokoyama, T., & Shimojo, M. 1996, ApJ, 464, 1016

Chiuderi-Drago, F., Mein, N., & Pick, M. 1986, Solar Phys., 103, 235

Kundu, M.R., Shibasaki, K., Enome, S., & Nitta, N. 1994, ApJ, 431, L155

Kundu, M.R., Raulin, J.P., Nitta, N., Hudson, H.S., Shimojo, M., Shibata, K., & Raoult, A. 1995, ApJ, 447, L135

Raulin, J.P., Kundu, M.R., Hudson, H.S., Nitta, N., & Raoult, A. 1996, A&A, 306, 299

Rust, D.M., Webb, D.F., & MacCombie, W. 1977, Solar Phys., 54, 53

Schmieder, B., van Driel-Gesztelyi, L., Gerlei, O., & Simnett, G.M. 1993, Solar Phys., 146, 163

Schmieder, B., Shibata, K., van Driel-Gesztelyi, L., & Freeland, S. 1995, Solar Phys., 156, 245